Life Sciences 231 (2019) 116537

Contents lists available at ScienceDirect

Life Sciences

journal homepage: www.elsevier.com/locate/lifescie

Vitamin D_3 increases the Caspase-3 p12, MTHFR, and P-glycoprotein reducing amyloid-β_{42} in the kidney of a mouse model for Down syndrome

Fabiana de Campos Gomes[a], João Simão de Melo-Neto[b], Merari de Fátima Ramires Ferrari[c], Carla Patrícia Carlos[d], Eny Maria Goloni-Bertollo[a], Érika Cristina Pavarino[a,*]

[a] Genetics and Molecular Biology Research Unit (UPGEM), São José do Rio Preto Medical School (FAMERP), São José do Rio Preto, SP, Brazil
[b] Institute of Health Sciences, Federal University of Pará (UFPA), Belém, PA, Brazil
[c] Department of Genetics and Evolutionary Biology, Biosciences Institute, University of São Paulo (USP), São Paulo, SP, Brazil
[d] Faceres School of Medicine (FACERES), São José do Rio Preto, SP, Brazil

ARTICLE INFO

Keywords:
Down syndrome
Amyloid-β
Vitamin D3
Kidney

ABSTRACT

Aims: Renal dysfunction has been reported in individuals with Down syndrome (DS); however, the causes and mechanisms involved remain unknown. Here, we present a proposal for how the triplication of the amyloid beta precursor protein (*APP*) and, mainly the amyloid β peptide 1–42 ($A\beta_{42}$) can favor the development of renal abnormalities in DS. We evaluated the effects of vitamin D_3 (VD_3) supplementation on morphofunctional aspects and the repercussions on the presence and localization of $A\beta_{42}$, methylenetetrahydrofolate reductase (MTHFR), caspase-3 p12, and P-glycoprotein (Pgp) in the renal tissue of DS mouse model.

Main methods: Twenty female mice (14-week-old) belonging to the B6EiC3Sn-Rb(12.Ts171665Dn)2Cje/CjeDnJ lineage were divided into four experimental groups (n = 5/group): common diet; trisomy (Ts) and wild-type (Wt); and high doses VD_3, $Ts_{(VD3)}$, and $Wt_{(VD3)}$. All the groups were treated for 10 weeks. At 24 weeks, the protocol experimental was interrupted. The kidney was weighed, collected, and processed for immunochemical analysis for $A\beta_{42}$, Caspase-3 p12, MTHFR, and Pgp proteins. All data were analyzed statistically.

Key findings: Our results showed that VD_3 promoted an increase in caspase-3 p12, MTHFR, and Pgp, and consequently contributed to reduced $A\beta_{42}$ in the renal tissue of a mouse model of DS. Furthermore, VD_3 treatment affected the plasma creatinine and urea levels and contributed to the attenuation of the dilation of Bowman's space observed in trisomic mice.

Significance: Finally, the results showed that VD_3 may activate specific mechanisms involved in reduced $A\beta_{42}$ and tissue repair in the kidneys of a mouse model for Down syndrome.

1. Introduction

Down Syndrome (DS) is a chromosomal abnormality caused by alteration in number of genes on chromosome 21 [1]. Gene overexpression has implications throughout the genome, resulting in several abnormal phenotypes [2–4]. Among the phenotypes, a wide variety of urogenital abnormalities, such as renal dysfunction, have been described in adults with DS [4–6]. There are limited of studies that address the causes of nephropathy in DS [5,6]. However, the mechanisms involved in the occurrence of these abnormalities remain unknown. In the brain, the exacerbated production of amyloid β peptide 1–42 ($A\beta_{42}$) has been found to favor the activation of pro-apoptotic mechanisms, including the participation of caspase-3 [7]. After a cascade of events, in an attempt to maintain cellular homeostasis, other mediators induce the activation of pathways that may affect the morphological structure and/or cause programmed cell death [8–10]. In the kidneys, the mechanisms involved in the exacerbated production of $A\beta_{42}$ have not been investigated in experimental models, and humans with DS.

Among the nephropathies described in DS, the presence of chronic renal failure may represent a risk for the appearance of other renal diseases [5,6,11]. Kidney failure may progress to chronic kidney disease (CKD), favoring the appearance of complications and comorbidities [12,13]. People with CKD, and curiously in DS, have a deficiency of vitamin D_3 (VD_3). The causes are associated with reduced VD_3 levels in the CKD and DS that are multifactorial, including a poor diet quality, reduced sun exposure [5,14], and particularly described for CKD, a loss

* Corresponding author at: Genetics and Molecular Biology Research Unit (UPGEM), São José do Rio Preto Medical School (FAMERP), Av. Brigadeiro Faria Lima, 554, São José do Rio Preto, SP CEP: 15090-000, Brazil.
E-mail address: erika@famerp.br (É.C. Pavarino).

https://doi.org/10.1016/j.lfs.2019.06.012
Received 20 February 2019; Received in revised form 30 May 2019; Accepted 5 June 2019
Available online 06 June 2019
0024-3205/

of 25-hydroxycholecalciferol in cases of proteinuria nephropathy [15].

Vitamin D [25(OH)D] is important for renal morphophysiology [16,17]. The kidney is also responsible for the synthesis of the active form of vitamin D (VD), 1,25-dihydroxyvitamin D3 [1,25 (OH)2D3] [18]. Through binding to the nuclear VD receptor (VDR), 1,25 (OH)2D3 activates transcriptional mediators and regulates genes responsive for VD. The calcitriol-receptor complex can regulate important mechanisms, including the increase in transport mediated by P-glycoprotein (Pgp), a membrane protein important in the clearance de $A\beta_{42}$ in brain tissue [19]; and in regulating receptors involved in folate transport [20]. Folate has a key role in cell growth and proliferation [21], and the levels of this metabolite are regulated by the enzyme methylenetetrahydrofolate reductase (MTHFR) [22]. Genetic variations of *MTHFR* are associated with the presence of nephropathy [23,24]. In addition, VD_3 may influence folate levels [25]. Therefore, although still unknown, MTHFR can be influenced by VD_3, and play an important role in renal morphophysiology.

Given the importance of VD_3 in the physiological functions, prevention and/or treatment of renal diseases, and its role in $A\beta_{42}$ clearance [10,26,27], we analyzed the effects of VD_3 supplementation in the morphological/functional parameters and repercussions on the presence and localization $A\beta_{42}$, MTHFR, caspase-3 p12, and Pgp proteins in the kidney of a mouse model for DS. For the first time, we characterized, before and after VD_3 supplementation, a relationship between immunolocalization and expression of proteins involved in pathogenic processes, tissue repair, apoptosis and clearance of Aβ amyloid in the kidney of a mouse model for DS.

2. Methods

2.1. Animals and experimental environment

Female mice (*Mus musculus*) of the lineage B6EiC3Sn-Rb (12.Ts17^{16}65Dn)2Cje/CjeDnJ (#004850) carrying a Robertsonian translocation [28] (The Jackson Laboratory, Bar Harbor, ME, USA) were maintained with normal diploid B6EiC3SnF1/J male for mating (both with 3-month-old). The offspring of B6EiC3Sn-Rb (12.Ts17^{16}65Dn)2Cje/CjeDnJ and B6EiC3SnF1/J mice were karyotyped at 21 days of age, according to protocol of instructions provided by The Jackson Laboratory (USA) to determine the presence of the trisomy, and subsequently distributed into control and experimental groups. The genotyping test was performed in the Biosciences Institute, University of São Paulo (USP), São Paulo, SP, Brazil. Throughout the experimental protocol, the mice were maintained in the Central Bioterium of the São José do Rio Preto Medical School (FAMERP) under adequate conditions of lighting (12-hour light-dark cycle) and temperature (23 ± 2 °C). The experiment protocol was approved by the Ethics Committee for Animal Use of the FAMERP, protocol n. 001-002447/2015. In the present study, only female offspring were used in the experimental protocol because the early pathophysiological mechanisms associated with Aβ have been reported more frequently in women with DS [29] and female Ts65Dn mice, a model for DS [30,31]; Therefore, knowledge about the role of peripheral clearance of Aβ in the kidney is extremely important.

2.2. Experimental groups

Initially all mice had access to a standard solid diet (Nuvilab®, Curitiba, PR, Brazil) and water *ad libitum*. With 14 weeks of age the animals were submitted to the experimental protocol. Female mice (14-week-old) were distributed in four experimental groups (n = 5/group) according to a presence (Ts) or absence of the trisomy (Wt) and supplemented with vitamin D_3 (VD_3) or control diet (CO) as follows: control diet with positive genotype ($Ts_{(CO)}$), control diet with negative genotype ($Wt_{(CO)}$), vitamin D_3 with positive genotype ($Ts_{(VD3)}$), vitamin D_3 with negative genotype ($Wt_{(VD3)}$).

2.3. Diet

The $Ts_{(CO)}$ and $Wt_{(CO)}$ groups were maintained with a standard diet throughout the experiment. Whereas, the mice of the $Wt_{(VD3)}$ and $Ts_{(VD3)}$ groups were fed a diet supplemented with high doses of VD_3 for 10 weeks (12,500 IU/kg, Domeneghetti & Corrêa Ltda®, Jaú, SP, Brazil), according to Wergeland et al. [32].

2.4. Euthanasia and tissue collection and processing

24-week-old mice were euthanized with high-dose 100 mg/kg sodium thiopental (Tiopental®), administered intraperitoneally according to animal weight. After total sedation, blood samples were collected. Posteriorly, transcardial perfusion was performed with phosphate-buffered saline solution (PBS) pH 7.4. Then, the kidneys (left antimer) were excised and weighed, fixed in 4% paraformaldehyde diluted in PBS, processed, and embedded in paraffin, cut into 5 µm thick sections. The slides followed for the morphometric and immunohistochemistry analyses.

2.5. Renal function analysis

The plasma samples were used to detect the following biochemical markers: plasma urea and creatinine (^{P}Cr). The samples of all groups were checked with colorimetric assay and analysis by spectrophotometry (BIO-200, Bioplus, São Paulo, SP, Brazil) using commercial kits (Biotécnica, Varginha, MG, Brazil).

2.6. Morphometric analysis

The slides were stained with hematoxylin-eosin (HE) and Bowman's space (µm), glomerulus diameter (µm), diameter of the renal corpuscles (µm), glomerular area (µm^2), and area of the renal corpuscles (µm^2) were analyzed. Fifteen microscopic fields were randomly selected (objective magnification 40×) per group. The analysis was performed in the Zeiss Primo Star microscope model coupled to a camera (Zeiss Axiocam 105 color model) and Zen Lite 2.3 software (Zeiss).

2.7. Immunohistochemistry analyses of $A\beta_{42}$, Pgp, MTHFR, and caspase-3 p12

The sections were deparaffinized, hydrated, and subjected to antigenic recovery. Posteriorly, submitted to endogenous peroxidase blocking and nonspecific proteins with skim milk (MOLICO®). The primary antibodies (abcam®, USA) used for incubation were: anti-beta Amyloid 1–42 (1:1000 concentration; ab201060), anti-P Glycoprotein (1:250 concentration; ab170904), anti-MTHFR (1:200 concentration; ab203789), and anti-caspase-3 p12 (1:500 concentration; ab179517). After overnight incubation with the primary antibodies, the sections were washed in PBS buffer and incubated with Goat antirabbit IgG H&L secondary antibodies (1:500 concentration, HRP, abcam®, USA, ab97051). Posteriorly, the slides were revealed with DAB chromogen and counterstained with hematoxylin. To confirm the specificity of the reaction, negative controls were used.

The analysis was performed in the renal cortex and medulla by photos acquired on the microscope Zeiss Primo Star model coupled to a camera (Zeiss Axiocam 105 color model) (objective magnification 20× and 40×) and Zen Lite 2.3 software (Zeiss), according Fu et al. [33]. Tissue area fields per group were randomly used to evaluate the percentage (%) of immunoreactivity. These fields were analyzed using ImageJ 1.47 software, windows version (National Institutes of Health, USA), according to Ruifrok and Johnston's method [34]. During the immunohistochemistry analysis, the fixed threshold was established to obtain of the percentage of the immunostained tissue area to the proteins analyzed.

2.8. Statistical analysis

Data were analyzed by descriptive and inferential statistics. The data were initially subjected to the Shapiro-Wilk normality test. The results were presented as mean and standard deviation or median and 95% confidence interval as appropriate for parametric or non-parametric tests. The following between-groups factors were considered for statistical analyses: presence of trisomy, vitamin D_3, and their interaction (trisomy and vitamin D_3). Two-way analysis of variance (ANOVA) with the *post hoc* Bonferroni test (parametric) or Scheirer Ray Hare test with the *post hoc* Mann-Whitney *U* test (non-parametric) were applied to assess group heterogeneity in the biometric parameters and renal function, morphometry, and percentage of immunoreactive area. The F-(F) and H-statistic (H) were presented to analyze between-groups factors (trisomy, vitamin D3, and their interaction). The effect of size (low 0.01 to 0.33; moderate 0.34 to 0.66; high 0.66 to 0.99) was analyzed for parametric data by eta partial squared analysis (ηp2). The probability of a Type I error for the statistical tests was evaluated at $p < 0.05$.

3. Results

3.1. Vitamin D3 supplementation reduces body and kidney weight in trisomic mice

Regardless of the positive or negative genotype for partial trisomy, the supplementation of VD_3 in high doses contributes to loss of body weight. The groups treated with VD_3 (trisomic or not) had a lower body weight than that of the controls. In addition, we observed that the relative weight of the kidney in ($Ts_{(CO)}$) mice is higher than that in ($Wt_{(CO)}$) mice, but not in control mice treated with VD3 ($Wt_{(VD3)}$) compared to that of control group ($Wt_{(CO)}$), suggesting the direct involvement of the trisomy factor in morphological alteration. After VD_3 treatment, the kidney absolute was reduced ($Ts_{(CO)}$ *versus* $Ts_{(VD3)}$ group), suggesting VD_3 is a protective factor contributing to this reduction (Table 1).

3.2. Supplementation of vitamin D3 reverts renal morphological parameters altered by trisomy

Morphometric analysis showed the presence of morphological alterations in the renal tissue of the trisomic mouse group. We identified a dilation of Bowman's space in the $Ts_{(CO)}$ group than that of the $Wt_{(CO)}$. Trisomy did not affect parameters, such as glomerular and renal corpuscle diameter/area ($Ts_{(CO)}$ *vs* $Wt_{(CO)}$). After VD_3 supplementation, it was observed the Bowman's space in $Ts_{(VD3)}$ group was reduced, an effect not observed in $Wt_{(VD3)}$ compared to that of the $Wt_{(CO)}$ group. In relation to the glomerular and renal corpuscle diameter/area, independent of genotype, VD_3 reduced these structures. For the glomerular area, a reduction was observed only in the $Wt_{(VD3)}$ group compared with that of the control ($Wt_{(CO)}$) (Table 1).

3.3. Vitamin D3 reduces plasma urea in trisomic mice

High-doses of VD_3 changed the ^{P}Cr and plasma urea levels in Ts and Wt groups. The urea level was reduced in $Ts_{(VD3)}$ and $Wt_{(VD3)}$ in comparison to that of their control groups. However, a significant increase in ^{P}Cr was observed in the $Ts_{(VD3)}$ *versus* $Ts_{(CO)}$ group, being trisomy factor responsible by increase of ^{P}Cr (Table 1).

3.4. Immunohistochemistry

3.4.1. Vitamin D_3 reduces the expression of β-amyloid peptide ($Aβ_{42}$) induced by trisomy in the kidney

In all experimental groups, we verified the presence of immunoreactivity to $Aβ_{42}$ (Fig. 1A–H). However, the distribution pattern and immunoreactivity of this protein differs among control and experimental groups. In $Ts_{(CO)}$ (Fig. 1A/E) *versus* $Wt_{(CO)}$ (Fig. 1C/G), we observed a high immunostaining for $Aβ_{42}$ in the renal cortex and medulla. This protein in the $Ts_{(CO)}$ group was localized in the glomerular tuft (cell nucleus and cytoplasm; and between the glomerular cells), proximal and distal tubules and blood vessels (veins, arteries, glomerular capillary), and renal tubular cells and vessels in the inner and outer medulla (Fig. 1A/E). Interestingly, in the medulla an intense deposition of $Aβ_{42}$ similar to that of the amyloid plaques was observed. In addition, we observed the presence of inflammatory infiltrate in the renal cortical interstice (Fig. 1B). However, VD_3 decreased the immunoreactivity area percentage for $Aβ_{42}$ in $Ts_{(VD3)}$ *versus* $Ts_{(CO)}$ (Fig. 1A/E and B/F) that was not observed in $Wt_{(VD3)}$ compared to $Wt_{(CO)}$. Unlike the control group, $Aβ_{42}$ in $Ts_{(VD3)}$ mice was visualized as small clusters in the glomerular tuft (extracellular and intracellular), interstitial space, and blood vessels; beyond the presence of inflammatory infiltrate (Fig. 1B). This result indicated that VD_3 is an important factor for reducing $Aβ_{42}$ accumulation (Fig. 1I–K).

3.4.2. Caspase-3 p12 is enhanced by vitamin D_3 in trisomic mice

We observed immunoreactivity to caspase-3 p12 intracellularly

Table 1
Biometric parameters, renal functional, and morphometric analyses in the kidney of the different groups.

	$Ts_{(CO)}$	$Ts_{(VD3)}$	$Wt_{(CO)}$	$Wt_{(VD3)}$	$p_{(Trisomy)}$	$p_{(Vitamin\ D3)}$	$p_{(Interaction)}$
Biometric parameters							
Body weight (kg)	0.024 (0.020–0.027)	0.020 (0.017–0.024)[a]	0.026 (0.022–0.030)	0.022 (0.019–0.025)[b]	0.102	0.027*	0.970
Kidney weight (g): absolute**	0.173 ± 0.020	0.126 ± 0.018[a]	0.143 ± 0.025	0.134 ± 0.022	0.290	0.010§	0.064
Kidney weight (OW/BW): relative**	7.360 ± 0.509[d]	6.227 ± 0.585	5.567 ± 0.754	6.062 ± 0.939	0.008§	0.334	0.022§
Functional analysis							
Plasma urea (mg/dL)	40.43 ± 4.293	21.24 ± 3.853[a]	50.65 ± 10.74	24.64 ± 2.799[b]	0.018§	< 0.0001§	0.181
Plasma creatinine (mg/dL)	0.359 (0.254–0.444)	0.410 (0.392–0.449)[a,c]	0.308 (0.191–0.384)	0.346 (0.294–0.399)	0.028*	0.059	0.488
Morphometry							
Bowman's space (μm)	12.72 (10.95–22.62)[d]	6.52 (5.72–9.31)[a]	5.89 (4.91–12.42)	7.00 (6.49–11.03)	0.072	0.078	0.004*
Glomerulus diameter (μm)	102.66 ± 14.40	81.63 ± 16.41[a]	104.82 ± 23.75	77.79 ± 16.66[b]	0.857	< 0.0001§	0.525
Diameter of the renal corpuscles (μm)	122.57 ± 17.47	93.81 ± 20.84[a]	118.27 ± 22.63	88.36 ± 19.36[b]	0.353	< 0.0001§	0.912
Glomerular area ($μm^2$)	8465 ± 1795	6446 ± 2113	8526 ± 2800	5020 ± 1871[b]	0.231	< 0.0001§	0.192
Area of the renal corpuscles ($μm^2$)	11,401 (10152–12,257)	7468.5 (6627.7–9916.8)[a]	10,129 (8705.9–12,232)	6807.6 (5148.5–7793)[b]	0.151	< 0.0001*	0.813

OW: Organ weight. BW: Body weight. Ts: presence of trisomy. Wt: absence of trisomy. CO: control diet. VD_3: vitamin D_3 diet. Interaction (trisomy and vitaminD_3) *$p < 0.05$, Scheirer–Ray–Hare test + Mann-Whitney post-test or §$p < 0.05$, two-way Anova + Bonferroni post-test as follows: [a]$Ts_{(VD3)}$ *vs* $Ts_{(CO)}$; [b]$Wt_{(VD3)}$ *vs* $Wt_{(CO)}$; [c]$Ts_{(VD3)}$ *vs* $Wt_{(VD3)}$; [d]$Ts_{(CO)}$ *vs* $Wt_{(CO)}$.

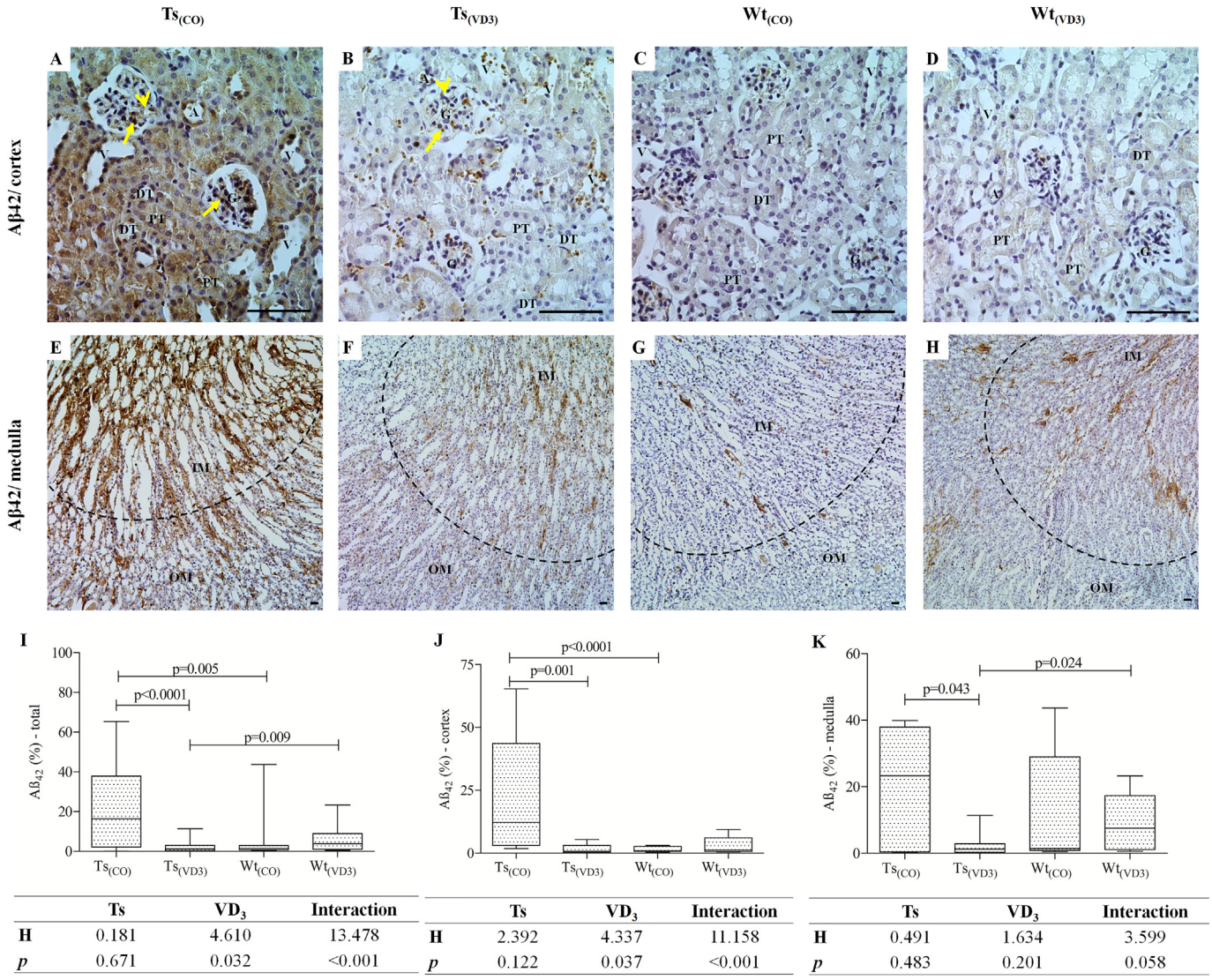

	Ts	VD_3	Interaction
H	0.181	4.610	13.478
p	0.671	0.032	<0.001

	Ts	VD_3	Interaction
H	2.392	4.337	11.158
p	0.122	0.037	<0.001

	Ts	VD_3	Interaction
H	0.491	1.634	3.599
p	0.483	0.201	0.058

Fig. 1. $A\beta_{42}$ immunolocalization. $A\beta_{42}$ protein was identified in renal cortex and medulla of the control and experimental groups [$Ts_{(CO)}$ (A, E), $Ts_{(VD3)}$ (B, F), $Wt_{(CO)}$ (C, G), $Wt_{(VD3)}$ (D, H)]. Kidney structures indicated as proximal tubule (PT), distal tubule (DT), glomerulus (G), veins (V), arteries (A), inner medulla (IM), outer medulla (OM). Black dashed circles delimitate medulla IM and OM; Yellow arrow indicates the presence of $A\beta_{42}$ in the cell nucleus and among glomerular cells; yellow arrowhead refers to the glomerular capillary. Inferential statistics of the semiquantitative analysis of the percentage (%) of coverage immunoreactive area: total (I), cortical (J) and medulla (K). Table: The H-statistic (H) for between-groups factors (trisomy, vitamin D_3 and interaction) was calculated on percentage (%) immunoreactive area in kidney. Scale-bars: 60 μm (A–D) and 20 μm (E–H), objective magnification 60× and 20×, respectively. (For interpretation of the references to color in this figure legend, the reader is referred to the web version of this article.)

(cytoplasm and nucleus) in the tubular system, medulla (inner and outer zones) and blood vessels (endothelial cells) in the kidney of the control and experimental groups (Fig. 2A–D and E–H). For the $Ts_{(VD3)}$ group, a discrete marking of caspase-3 p12 was observed in the glomerular tuft. Although the localization pattern for caspase-3 p12 was similar among groups, it was possible to observe perceptible differences in the percentage and intensity of the immunoreaction. The $Ts_{(CO)}$ group *versus* $Wt_{(CO)}$ has a lower immunoreaction for caspase-3 p12 in the renal medulla (Fig. 2K). However, the VD_3 induced an increase in caspase-3 p12 in the total kidney, cortex, and medulla in $Ts_{(VD3)}$ *versus* $Ts_{(CO)}$; this protein was visualized in the cytoplasm and nucleus of a large number of cells (Fig. 2B and F). Unlike, $Wt_{(VD3)}$ group presented a lower caspase-3 p12-immunoreactive percentage than that of $Wt_{(CO)}$ (Fig. 2I–K).

3.4.3. *Vitamin D_3 enhanced P-glycoprotein (Pgp) in the renal cortex*

In the kidney, a similar pattern of immunolocalization for Pgp was observed among the control and experimental groups (Fig. 3A–D). Pgp was localized in the cortical region, specifically in the proximal tubular cells (brush border membrane). Although the localization of Pgp was similar among groups, a significant increase in the percentage of the immunoreactive area was observed in $Ts_{(VD3)}$ *versus* $Ts_{(CO)}$ and $Wt_{(VD3)}$ *versus* $Wt_{(CO)}$ (Fig. 3B and D). There was no difference between $Ts_{(CO)}$ and $Wt_{(CO)}$ or between $Ts_{(VD3)}$ and $Wt_{(CO)}$ (Fig. 3E).

3.4.4. *Methylenetetrahydrofolate reductase (MTHFR) is enhanced by vitamin D_3 in trisomic mice*

In the renal tissue of trisomic and wild-type mice, MTHFR was immunolocalized in cytoplasm and/or cell membranes in the cortical region, including Bowman's capsule (membrane basement and parietal cells) and proximal convoluted tubule epithelial cells (cytoplasm and brush border membrane) near the renal corpuscle (Fig. 4A–D). A high intensity of MTHFR was observed in the parietal layer of the Bowman's capsule in $Wt_{(CO)}$. In renal tissue of the $Ts_{(VD3)}$ mice, it was possible to observe the intracellular presence of MTHFR in the parietal cells (Fig. 4B) at a higher magnification. Regarding immunoreactivity, we

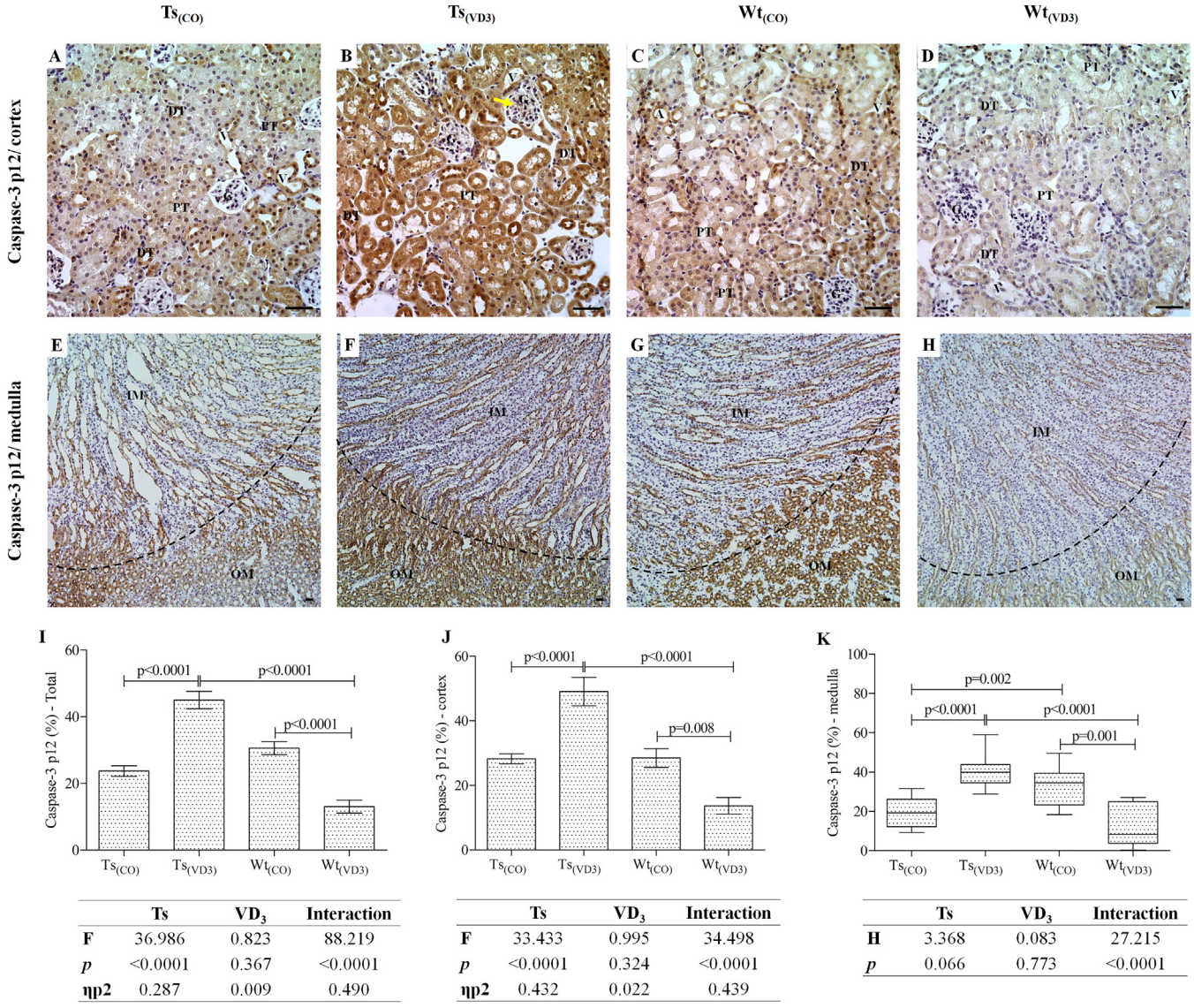

	Ts	VD_3	Interaction
F	36.986	0.823	88.219
p	<0.0001	0.367	<0.0001
ηp2	0.287	0.009	0.490

	Ts	VD_3	Interaction
F	33.433	0.995	34.498
p	<0.0001	0.324	<0.0001
ηp2	0.432	0.022	0.439

	Ts	VD_3	Interaction
H	3.368	0.083	27.215
p	0.066	0.773	<0.0001

Fig. 2. Caspase-3 p12 immunolocalization. Renal cortex and medulla of the control and experimental groups [$Ts_{(CO)}$ (A, E), $Ts_{(VD3)}$ (B, F), $Wt_{(CO)}$ (C, G), $Wt_{(VD3)}$ (D, H)] have caspase-3 p12 expression. Kidney structures indicated as proximal tubule (PT), distal tubule (DT), glomerulus (G), veins (V), arteries (A), inner medulla (IM), outer medulla (OM). Yellow arrow indicates glomerular tuft. Black dashed circles delimitate medulla IM and OM. Inferential statistics of the semiquantitative analysis of the percentage (%) of coverage immunoreactive area: total (I), cortical (J) and medulla (K). Table: The F-statistic (F), partial eta squared (np2) and H-statistic (H) for between-groups factors (trisomy, vitamin D_3 and interaction) were calculated on percentage (%) immunoreactive area in kidney. Scale-bars: 40 μm (A–D) and 20 μm (E–H), objective magnification 40× and 20×, respectively. (For interpretation of the references to color in this figure legend, the reader is referred to the web version of this article.)

observed an increase in MTHFR in $Ts_{(VD3)}$ *versus* $Ts_{(CO)}$ and $Ts_{(VD3)}$ *versus* $Wt_{(VD3)}$, but not in $Wt_{(VD3)}$ *versus* $Wt_{(CO)}$ (Fig. 4E).

4. Discussion

In DS, the presence of kidney abnormalities may compromise the renal function and favors the emergence of complications and co-morbidities. Although it has been reported that congenital abnormalities may be related the malformations in kidney [35], the causes of these events remain unknown. Taking into consideration that adults individuals with DS present renal abnormalities [4–6,36] and develop early-onset Alzheimer's disease (EODA) associated, mainly, to the increased Aβ accumulation [37]; and that elevated serum Aβ levels may be associated with a renal failure [38,39], being the kidney one of the main organs involved in peripheral clearance of Aβ peptides [40]; the knowledge about the presence and localization of the $Aβ_{42}$ protein in the kidney of a mouse model for DS is of great importance.

Several studies have shown that the VD_3 acts in the activation of mechanisms involved in the degradation and clearance Aβ peptides [19,41], and that diets enriched with VD_3 may help in the prevention or treatment of kidney diseases [15,42,43]. In this study we analyzed the effect of high-doses of VD_3 in kidney of adult female Rb (12.Ts17[16]65Dn)2Cje mice. Our findings showed an association between the localization and quantitative presence of Pgp, MTHFR, and Caspase-3 p12 proteins in response to VD_3 treatment and an increase in $Aβ_{42}$ peptides in the kidney.

The $Aβ_{42}$, Pgp, MTHFR, and Caspase-3 p12 proteins are modulated according VD_3 availability [7,19,25,26], and are involved in pathogenic processes; clearance; DNA repair and cell survival; and apoptosis, respectively [7,19,22]. The increased protein $Aβ_{42}$ may favor the activation of pathways that induce DNA damage and apoptosis leading to cell death [44]; therefore, it is fundamental to analyze these proteins in this context.

For the first time, our research showed the localization and

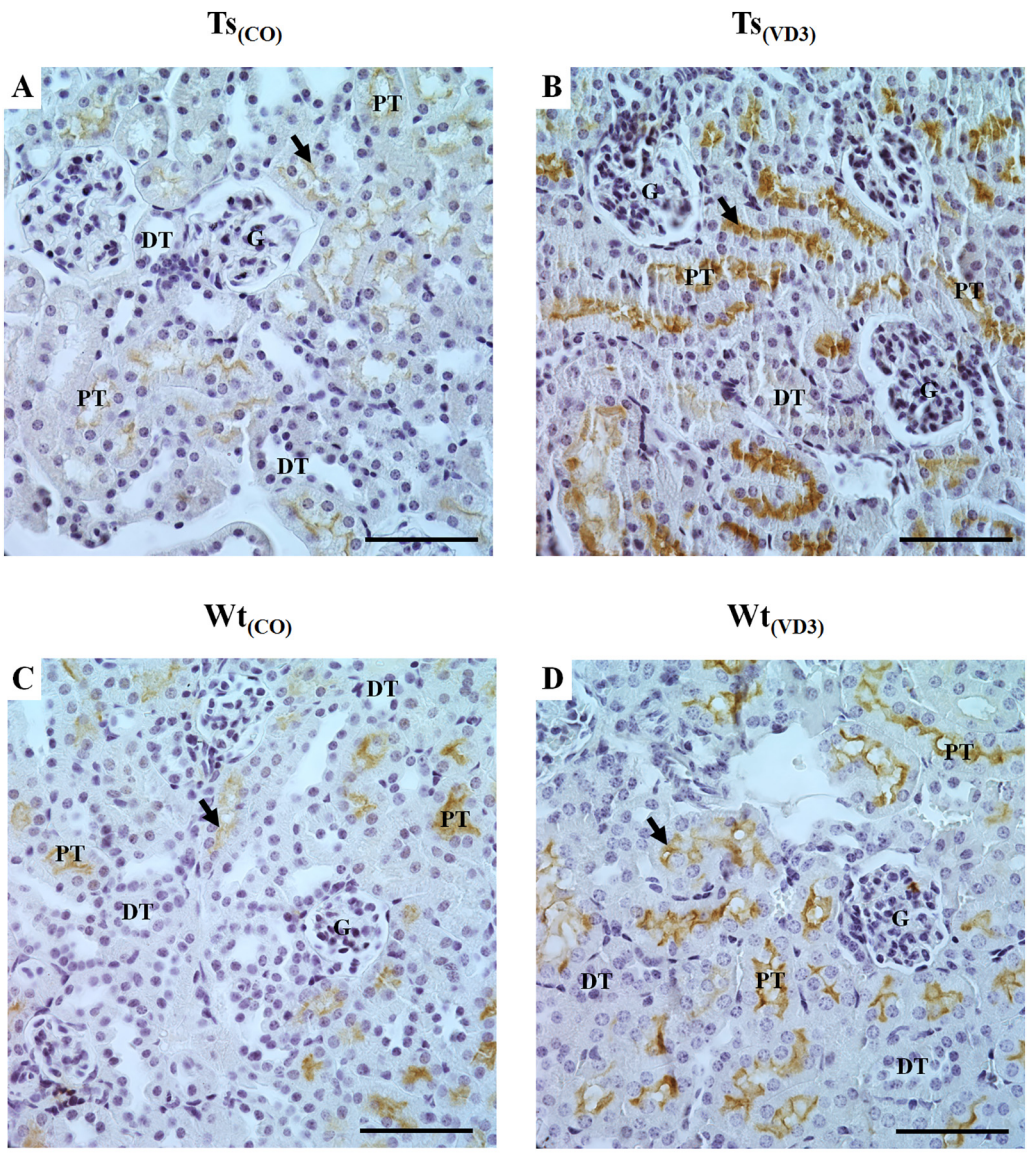

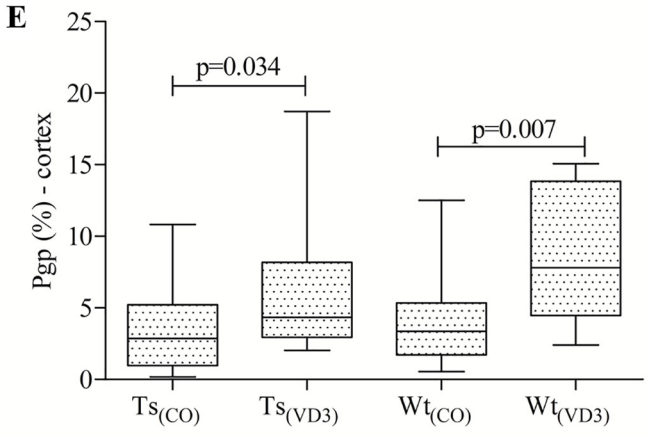

	Ts	VD_3	Interaction
H	1.430	8.696	0.225
p	0.232	0.003	0.635

Fig. 3. Pgp immunolocalization. (A–D, scale-bars 60 μm) identified in the renal cortex of the control and experimental groups [$Ts_{(CO)}$ (A), $Ts_{(VD3)}$ (B,), $Wt_{(CO)}$ (C), $Wt_{(VD3)}$ (D)]. Kidney structures indicated as proximal tubule (PT), distal tubule (DT), glomerulus (G). Black arrow indicates brush borders of proximal tubular cells. Objective magnification 40×, 60× and 100×. Inferential statistics of the semi-quantitative analysis of the percentage (%) of coverage immunoreactive area of cortical Pgp (E) in the kidney of the different groups. Table: The H-statistic (H) for between-groups factors (trisomy, vitamin D_3 and interaction) was calculated on percentage (%) immunoreactive area in kidney. Scale-bars: 60 μm, objective 60×.

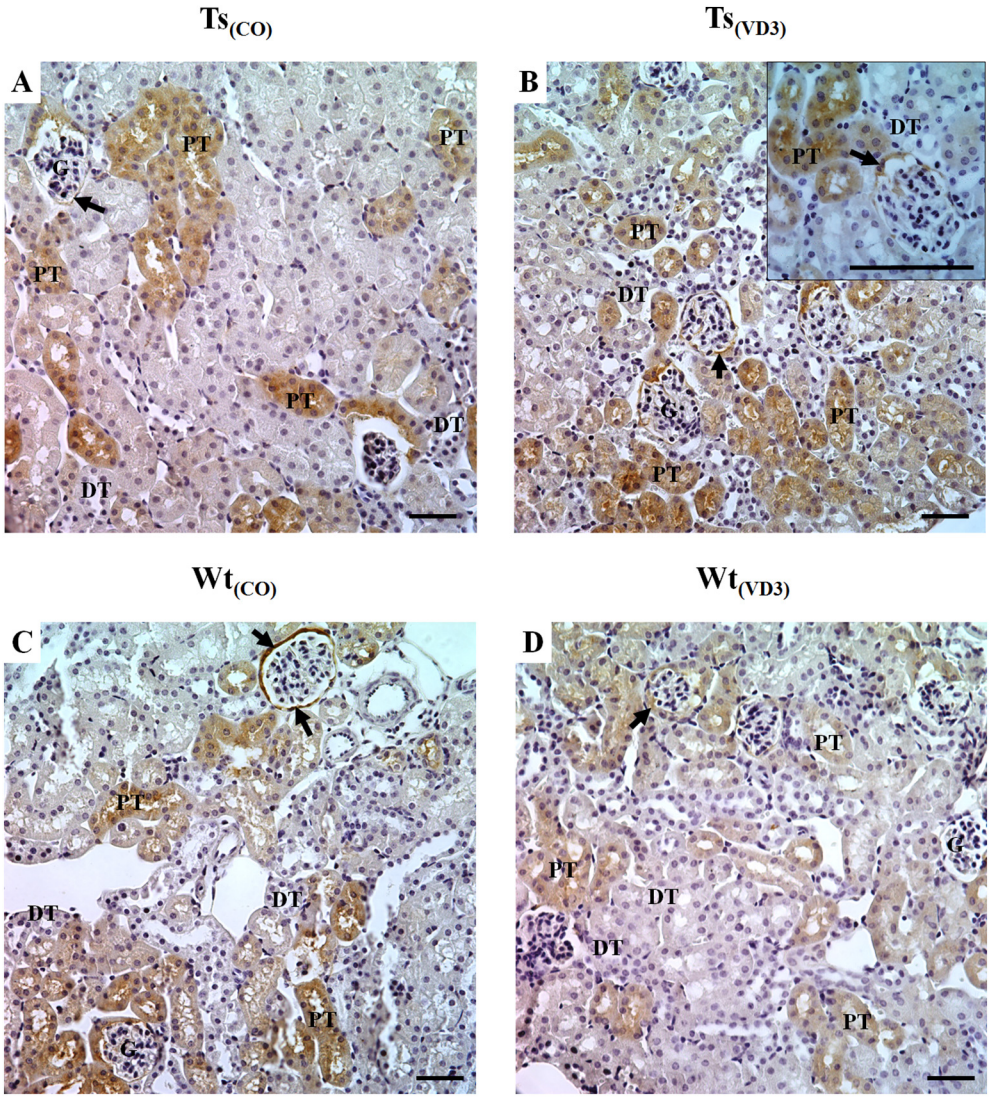

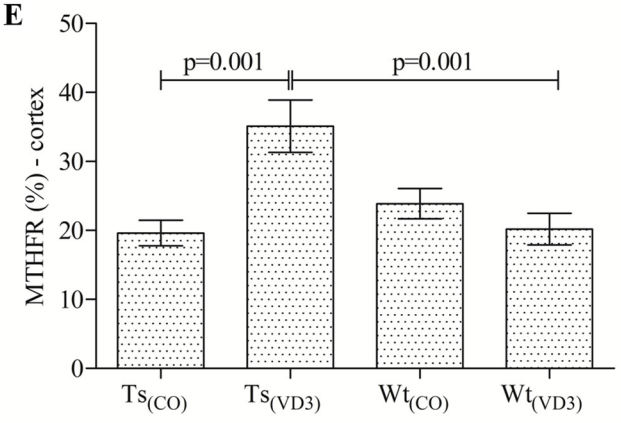

	Ts	VD_3	Interaction
F	4.091	4.997	13.215
p	0.049	0.031	0.001
ηp2	0.085	0.102	0.231

Fig. 4. MTHFR immunolocalization. Renal cortex of the control and experimental groups [$Ts_{(CO)}$ (A), $Ts_{(VD3)}$ (B), $Wt_{(CO)}$ (C), $Wt_{(VD3)}$ (D)] presents expression of MTHFR. Kidney structures indicated as proximal tubule (PT), distal tubule (DT), glomerulus (G). Black arrow indicates the presence of MTHFR in the Bowman's capsule (parietal layer). In higher magnification (detail in B), it is possible to observe the intracellular presence of MTHFR in parietal cells. Inferential statistics of the semiquantitative analysis (E) of the percentage (%) of coverage immunoreactive area of cortical MTHFR in the kidney of the different groups. Table: The F-statistic (F), partial eta squared (np2) for between-groups factors (trisomy, vitamin D_3 and interaction) were calculated on percentage (%) immunoreactive area in kidney. Scale-bars: 40 μm (A–D) and 100 μm (B), objective magnification 40× and 100×, respectively.

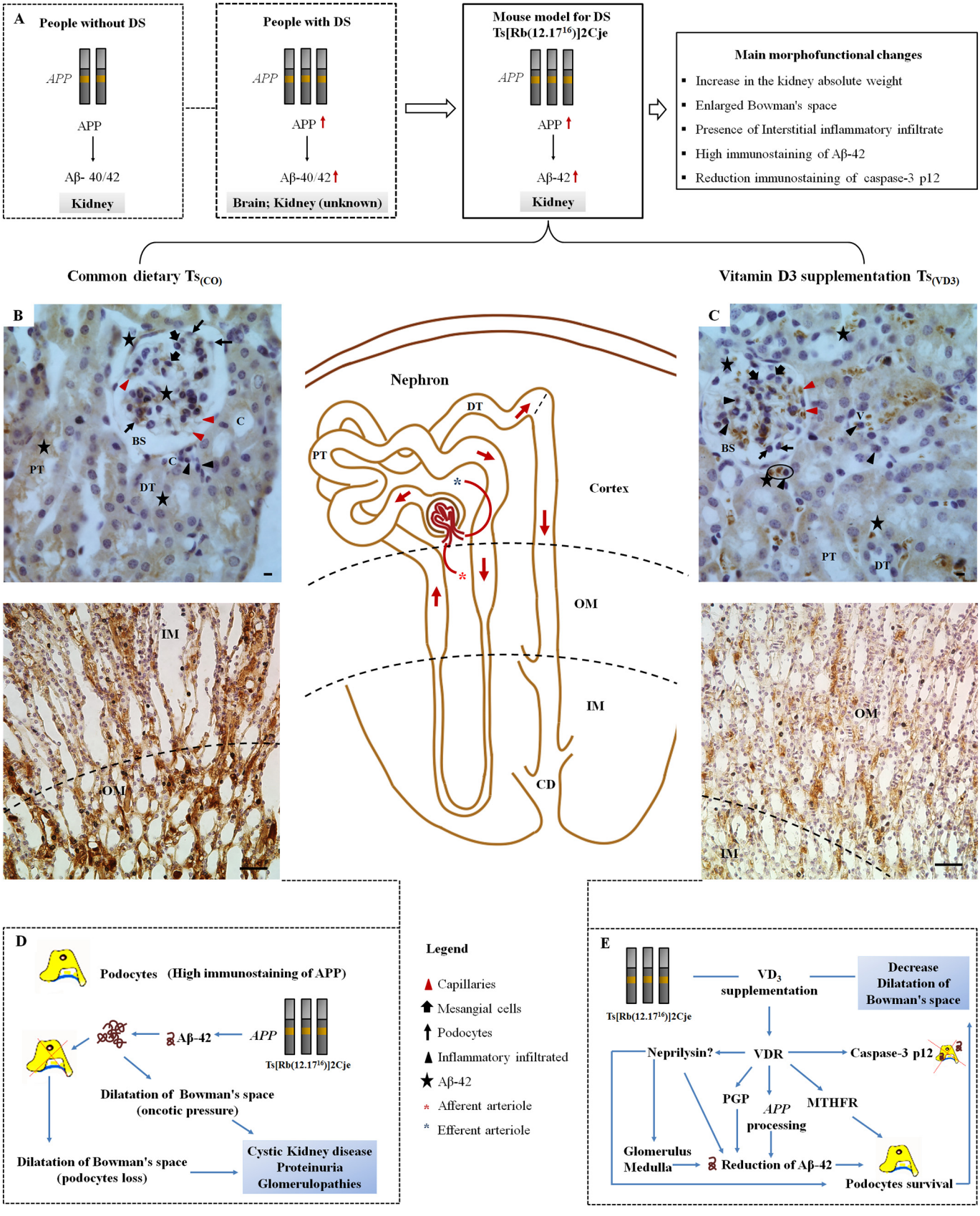

(caption on next page)

Fig. 5. Proposed model for how the overexpression of *APP* and its product, $A\beta_{42}$, may favor the appearance of renal tissue abnormalities in DS mouse model and human trisomy 21. A. APP protein and Aβ- 40/42 peptides (immunostained) (white box) has been observed in kidneys of people without Down syndrome (DS) [45]. In DS individuals and mice models, it has been well-described that *APP* overexpression results in increased levels of Aβ- 40/42 (red arrow) in the brain [46]. However, its expression pattern remains unknown in the kidney. In our study with DS mouse model Ts[Rb(12.17^{16})]2Cje, the overexpression of *APP* [28] and increased of $A\beta_{42}$ are associated with morphofunctional changes. B and C. Presence and location of $A\beta_{42}$ in the kidney of $Ts_{(CO)}$ and $Ts_{(VD3)}$ mice. The renal cortex and medulla of both groups (between C and D) when compared to the nephron scheme show structural delimitations. This provides an indication of how $A\beta_{42}$ protein can affect the functional unit of the kidney. The red arrows in the figure (nephron) indicate the blood flow in the vessels from the afferent and efferent arteriole. Kidney structures are indicated as Bowman's space (BS), proximal tubule (PT), distal tubule (DT), glomerulus (G), outer medulla (OM), inner medulla (IM), and collecting duct (CD). Black dashed circles delimitate IM and OM. Other symbols used are explained in the legend box. B and C scale-bars are 10 and 40 μm, respectively (objective magnification 40× and 100×). D. Mechanism proposed by which *APP* overexpression and increase in $A\beta_{42}$ may be involved in renal abnormalities. In rats, APP is immunolocalized in podocytes with an important role in the glomerular filtration [49]. In the $TS_{(CO)}$ mice, the agglomeration and nuclear localization of $A\beta_{42}$ in podocytes suggest a crucial point to initiate events that can induce cell death, contributing to the dilation of BS. $A\beta_{42}$ can also accumulate in the BS and increase the oncotic pressure. Possibly a deregulation caused by increased $A\beta_{42}$ may be involved with some nephropathies reported in individuals with DS (blue box). E. Proposed mechanism by which VD_3 can act on clearance of $A\beta_{42}$ in the kidney of Ts mice. The active form of VD_3 binds to the VDR receptor and can induce the expression of genes that regulate or are involved in the expression of proteins, such as Pgp and possibly neprilysin enzymes that participate clearance of $A\beta_{42}$. VD_3 may also induce the increase of caspase-3 p12 and/or promote the increase of MTHFR contributing to cell proliferation and survival (blue arrows). After the activation of specific mechanisms [19,41,52] several events occur favoring the reduction of $A\beta_{42}$ and cell survival (blue arrow). (For interpretation of the references to color in this figure legend, the reader is referred to the web version of this article.)

accentuated presence of $A\beta_{42}$ in the kidney of a DS mouse model. These findings strengthen the supposition that increased $A\beta_{42}$ can be involved with the dilation of the Bowman's space (BS) in $Ts_{(CO)}$ mice, and it is possible a similar condition may occur in people with DS. Owing limited information about factors involved in the renal abnormalities in DS, and based on the literature [29,37–39,45–47], we hypothesized that the overexpression of *APP* and, mainly the $A\beta_{42}$ protein, may be involved with abnormalities reported in the renal tissue of individuals with DS and experimental models. This proposal, as well as the involved action mechanisms [1,19,45,46,48–52] are presented in Fig. 5.

After treatment with high-doses of VD_3, the decrease in $A\beta_{42}$ was accompanied by a reduction in BS in $Ts_{(VD3)}$ similarly to parameters in Wt mice. In humans, the enlarged BS in the kidneys of DS individuals is associated with a nephropathology, known as cystic and glomerulocystic kidney disease [53,54,63,64]. Therefore, in DS, considering these kidney diseases and risk of complications, interventions that could attenuate the progression of the disease are of extreme importance.

In addition, the presence of $A\beta_{42}$ in the glomerular capillaries, veins and medulla, suggests that this protein comes from systemic circulation. Previously, it was described that in humans and mice, the blood Aβ levels are lower in the inferior vena cava than in the femoral artery, indicating Aβ effluxes of the brain to peripheral blood, which reinforces our hypothesis [40]. In addition, these authors [40] demonstrated that there is a peripheral clearance of brain-derived Aβ.

Although treatment with high-dose VD_3 reduced $A\beta_{42}$, adverse effects in the kidneys of $Ts_{(VD3)}$ and $Wt_{(VD3)}$ mice were observed. Among the adverse effects, a reduction in body weight was noted in groups treated with VD_3. Experimental studies in humans and mice also observed a body weight loss after VD_3 supplementation [44,55,56]. The mechanism by which VD_3 can reduce body weight might be related to lipid metabolism [51,57]. These findings suggested the existence of feedback between the supplementation and need to store VD_3 [51,52,58], as show in the Fig. 6.

Additionally, VD_3 promotes structural alterations in the kidneys. These morphological changes were accompanied by a reduction in caspase-3 p12 in $Wt_{(VD3)}$ and increase in $Ts_{(VD3)}$ groups. Caspase-3 is an important mediator for cellular apoptosis in the kidneys [10]. Here, we analyzed caspase-3 p12 to investigate alternative pathways, because depending on the stimulus, complexes involved in inflammation and apoptosis, such as p17/p12 or p19/p12, can be formed [8]. The activation of caspase 3 is a critical step in the pathways that lead to morphological and biochemical alterations [9]. Based on these studies, a reduction in caspase-3 p12 in $Wt_{(VD3)}$ could indicate the participation of other cellular mechanisms in an attempt to inhibit the apoptosis or pro-inflammatory pathway activation.

In $Ts_{(VD3)}$ mice in response to intrinsic increased $A\beta_{42}$, a high immunoreactivity of caspase-3 p12 may be related to the reversion of morphological changes, as Bowman's space dilation and enhanced relative kidney weight, as previously observed in the $Ts_{(CO)}$. Caspase 3 also has an important role in the cleavage APP protein [59], consequently this can affect $A\beta_{42}$ deposition and apoptosis. For $Ts_{(CO)}$ adult mice, we did not find a relationship between the increase in $A\beta_{42}$ and caspase-3 p12. However, the presence of small clusters of inflammatory cells in the interstitial space (Fig. 5B) may indicate an early-stage response, which over time may progress to complications and affect the kidney morphophysiology.

In parallel with the morphofunctional changes, the Ts factor and high-dose VD_3 also affect plasma creatinine and urea concentration. The alterations in urea and creatinine levels in relation to the normal limit refers to variations in glomerular filtration rate and tubular function [60,61], and may be associated with renal dysfunction. Despite the VD_3 protective effect to reverse increased urea levels in Ts mice, an elevation in the creatinine level in the group treated with VD_3 was observed, the opposite effect when compared to urea in this group. It is possible that at the time of the animal sacrifice, 10 weeks after the initiation of experiments and treatments, VD_3 worsened the creatinine level, despite improvement in the urea excretion and simultaneous renal structure. Therefore, this effect could be improved with an extended VD_3 treatment. It is interesting to verify the kidney function by assessing glomerular filtration at different times of treatment with VD_3. Therefore, although the VD_3 plays an important role in several mechanisms, such as the reduction in $A\beta_{42}$ in the cerebral tissue [19,50,62], more research is needed, especially to assess the adverse effects in peripheral organs, such as the kidneys.

In addition, the data in relation to urea levels showed an association between increased Pgp in the brush border of apical membrane of proximal tubular epithelial cells and reduction urea levels in trisomic and non-trisomic groups that received VD_3 (Fig. 6). Still, the increase in Pgp contributed to reduced $A\beta_{42}$ in the kidneys of $Ts_{(VD3)}$ mice in the present study. Pgp plays an important role in $A\beta_{42}$ clearance in cerebral tissue [63]. Studies with mice show that VD_3 supplementation increases Pgp immunostaining and expression with reduced amounts of $A\beta_{42}$ in the brain [19]. This suggests that mechanisms similar to those observed in the brain [41,50,52] also occur in the kidney and others in according to the Fig. 5D and E.

Besides these mechanisms, increased MTHFR in $Ts_{(VD3)}$ the kidneys seems to further support the role of VD_3 in the morphological restoration (Fig. 6). To the best of our knowledge, we are the first to show the immunolocalization of MTHFR in the renal tissue of trisomic and non-trisomic mouse DS models. MTHFR is important in the process of folate metabolism regulation, which is involved in nucleotide synthesis, DNA replication, cell growth, and survival [22,64]. The presence of MTHFR in the proximal tubule epithelial cells (cytoplasm and brush-border

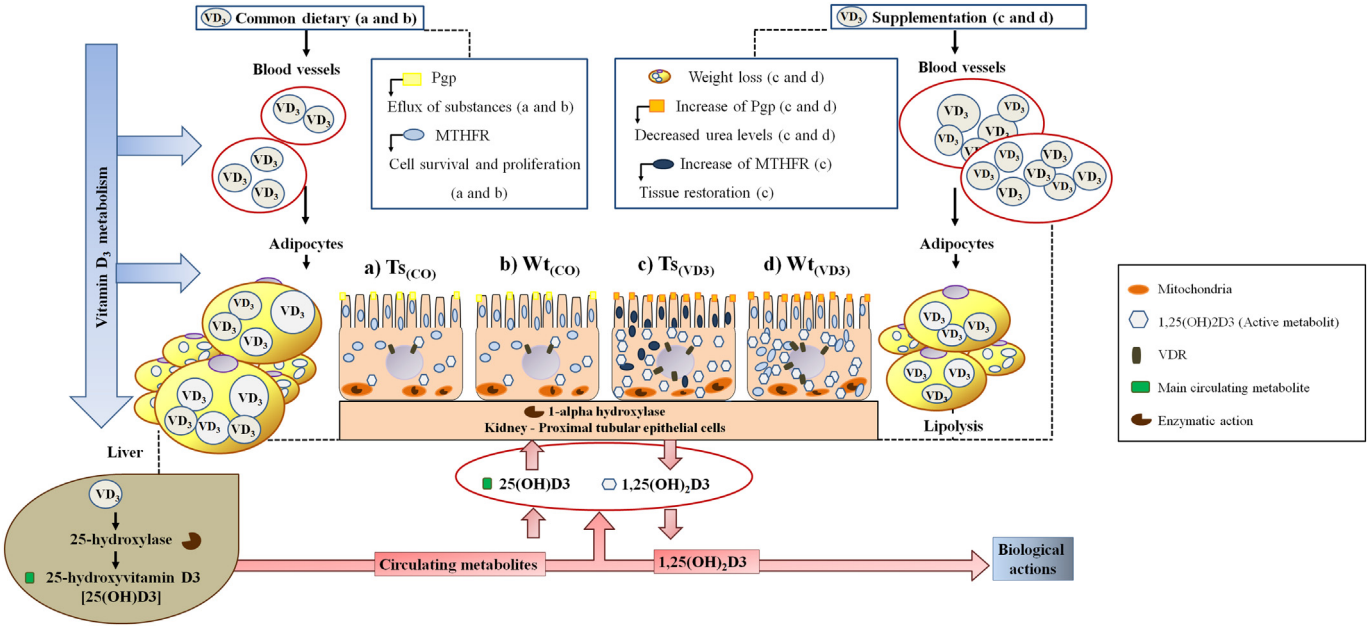

Fig. 6. Scheme proposed for the interactions between Pgp and MTHFR proteins in kidney of Ts and Wild-type mice. The VD_3 from a standard diet or supplementation are incorporated into cytochrome and transported through the blood vessels. VD_3 can be stored and released by adipocytes. Circulating VD_3 is transported to the liver and converted into 25-hydroxyvitamin D3 [25(OH)D3] by the enzyme, 25-hydroxylase. 25(OH)D3 is the primary circulating metabolite. In kidneys, specifically in the mitochondria of proximal tubule epithelial cells, 25(OH)D3 is converted by the enzyme 1-alpha hydroxylase into its active form 1,25(OH)2D3, that has biological action [18,51,58]. Our findings suggest that supplementation causes a high availability of VD_3 and reduces the need for storage, leading to increased lipolysis and thus resulting in body weight loss (c–d). VD_3 supplementation may result in increased levels of 1,25(OH)2D3 that can bind to the nuclear receptor VDR, favoring the increase in Pgp (c–d) and possibly with the reduction of urea levels. Notably, the increase in MTHFR is observed only in Ts treated with VD_3. Possibly, this protective role may be due to increased intrinsic $A\beta_{42}$, and therefore, there is a greater need for VD_3-responsive mechanisms [19,52].

membrane) and in Bowman's capsules (basement membrane and parietal cells) indicate that this protein may be involved in mechanisms of cell proliferation and survival, such as podocytes and tissue restoration, contributing to a reduced Bowman's space in $TS_{(VD3)}$ mice, similarly to the standard parameters, as observed in wild-type mice.

5. Conclusion

Supplementation with high-dose VD_3 affects renal morphophysiology and attenuates Bowman's space dilation in the kidney of adult female mice model for DS. Moreover, VD_3 supplementation influences the presence and localization of caspase-3 p12, Pgp, and MTHFR proteins and contributes to reduced $A\beta_{42}$.

Thus, this research can contribute to new studies and perspectives for a better understanding of the possible causes of nephropathies in individuals with DS and the role of kidney in the peripheral clearance of $A\beta_{42}$, as well as possible implications involved in the development of EOAD in DS. In addition, the use of high doses of VD_3 requires further investigation to determine if VD_3 supplementation could lead to adverse implications in renal morphophysiology.

Declaration of Competing Interest

The authors have declared that have no conflicts of interest.

Acknowledgments

This study was financed in part by Coordenação de Aperfeiçoamento de Pessoal de Nível Superior – CAPES - Finance Code 001 and Conselho Nacional de Desenvolvimento Científico e Tecnológico (CNPq) grant numbers: 310806/2018-6. We thank the Laboratory of Experimental Immunology and Transplantation (Litex), Laboratory of histotechnology of the São José do Rio Preto Medical School (FAMERP) and Department of Biology, Laboratory of Microscopy and Microanalysis, Paulista State University/UNESP by technical support.

References

[1] S.E. Antonarakis, R. Lyle, E.T. Dermitzakis, et al., Chromosome 21 and down syndrome: from genomics to pathophysiology, Nat. Rev. Genet. 5 (10) (2004) 725–738.
[2] J.R. Korenberg, X.N. Chen, R. Schipper, et al., Down syndrome phenotypes: the consequences of chromosomal imbalance, Proc. Natl. Acad. Sci. U. S. A. 91 (11) (1994) 4997–5001.
[3] S.E. Antonarakis, Down syndrome and the complexity of genome dosage imbalance, Nat. Rev. Genet. 18 (3) (2017) 147–163.
[4] C. Stoll, B. Dott, Y. Alembik, et al., Associated congenital anomalies among cases with Down syndrome, Eur. J. Med. Genet. 58 (12) (2015) 674–680.
[5] S. Málaga, R. Pardo, I. Málaga, et al., Renal involvement in Down syndrome, Pediatr. Nephrol. 20 (5) (2005) 614–617.
[6] V.B. Kute, A.V. Vanikar, P.R. Shah, et al., Down syndrome with end-stage renal disease, Indian J. Clin. Biochem. 28 (4) (2013) 429–432.
[7] X.J. Han, Y.Y. Hu, Z.J. Yang, et al., Amyloid β-42 induces neuronal apoptosis by targeting mitochondria, Mol. Med. Rep. 16 (4) (2017) 4521–4528.
[8] E. Kavanagh, J. Rodhe, M.A. Burguillos, et al., Regulation of caspase-3 processing by cIAP2 controls the switch between pro-inflammatory activation and cell death in microglia, Cell Death Dis. 5 (12) (2014) e1565.
[9] P. Tawa, K. Hell, A. Giroux, et al., Catalytic activity of caspase-3 is required for its degradation: stabilization of the active complex by synthetic inhibitors, Cell Death Differ. 11 (4) (2004) 439–447.
[10] C.S. Kim, S.W. Kim, Vitamin D and chronic kidney disease, Korean J. Intern. Med. 29 (4) (2014) 416–427.
[11] S.M. Said, L.D. Cornell, S. Sethi, et al., Acquired glomerular lesions in patients with Down syndrome, Hum. Pathol. 43 (1) (2012) 81–88.
[12] M.S. Parmar, Chronic renal disease, BMJ 325 (7355) (2002) 85–90.
[13] E. Yen, N.F. Miele, J.G. Barone, et al., Untethering an unusual cause of kidney injury in a teenager with Down syndrome, Pediatr. Emerg. Care 30 (11) (2014) 826–828.
[14] P. Zubillaga, A. Garrido, I. Mugica, et al., Effect of vitamin D and calcium supplementation on bone turnover in institutionalized adults with Down's syndrome, Eur. J. Clin. Nutr. 60 (5) (2006) 605–609.
[15] J.E. Pena-Polanco, L.F. Fried, Established and emerging strategies in the treatment of chronic kidney disease, Semin. Nephrol. 36 (4) (2016) 331–342.
[16] Y.C. Li, Podocytes as target of vitamin D, Curr. Diabetes Rev. 7 (1) (2011) 35–40.
[17] Y. Wang, M.L. Borchert, H.F. DeLuca, Identification of the vitamin D receptor in various cells of the mouse kidney, Kidney Int. 81 (10) (2012) 993–1001.
[18] M.F. Holick, Vitamin D deficiency, N. Engl. J. Med. 357 (2007) 266–281.
[19] M.R. Durk, K. Han, E.C. Chow, et al., 1α,25-Dihydroxyvitamin D3 reduces cerebral

amyloid-β accumulation and improves cognition in mouse models of Alzheimer's disease, J. Neurosci. (21) (2014) 7091–7101.
[20] C. Alam, M.T. Hoque, R.H. Finnell, et al., Regulation of reduced folate carrier (RFC) by vitamin D receptor at the blood-brain barrier, Mol. Pharm. 14 (11) (2017) 3848–3858.
[21] I. Abe, K. Shirato, Y. Hashizume, et al., Folate-deficiency induced cell-specific changes in the distribution of lymphocytes and granulocytes in rats, Environ. Health Prev. Med. 18 (1) (2012) 78–84.
[22] D. Leclerc, S. Sibani, R. Rozen, Molecular biology of methylenetetrahydrofolate reductase (MTHFR) and overview of mutations/polymorphisms, Madame Curie Bioscience Database [Internet], Landes Bioscience, Austin (TX), 2000–2013Available from https://www.ncbi.nlm.nih.gov/books/NBK6561/.
[23] M.P. de Alvarenga, E.C. Pavarino-Bertelli, M. Abbud-Filho, et al., Combination of angiotensin-converting enzyme and methylenetetrahydrofolate reductase gene polymorphisms as determinant risk factors for chronic allograft dysfunction, Transplant. Proc. 39 (1) (2007) 78–80.
[24] Y. Long, J. Nie, Homocysteine in renal injury, Kidney Dis. (Basel) 2 (2) (2016) 80–87.
[25] M. Lucock, R. Thota, M. Garg, et al., Vitamin D and folate: a reciprocal environmental association based on seasonality and genetic disposition, Am. J. Hum. Biol. 30 (5) (2018) e23166.
[26] K. Mirković, J. van den Born, G. Navis, et al., Vitamin D in chronic kidney disease: new potential for intervention, Curr. Drug Targets 12 (1) (2011) 42–45.
[27] Y. Namir, M.J. Cohen, Y.S. Haviv, et al., Vitamin D levels, vitamin D supplementation, and prognosis in patients with chronic kidney disease, Clin. Nephrol. 86 (10) (2016) 165–174.
[28] A.J. Villar, P.V. Belichenko, A.M. Gillespie, et al., Identification and characterization of a new Down syndrome model, Ts[Rb(12.1716)]2Cje, resulting from a spontaneous Robertsonian fusion between T(171)65Dn and mouse chromosome 12, Mamm. Genome 16 (2) (2005) 79–90.
[29] N. Schupf, J.H. Lee, D. Pang, et al., Epidemiology of estrogen and dementia in women with Down syndrome, Free Radic. Biol. Med. (2017) 31.
[30] A.C. Granholm, K.A. Ford, L.A. Hyde, et al., Estrogen restores cognition and cholinergic phenotype in an animal model of Down syndrome, Physiol. Behav. 77 (2–3) (2002) 371–385.
[31] A.C. Granholm, L. Sanders, H. Seo, et al., Estrogen alters amyloid precursor protein as well as dendritic and cholinergic markers in a mouse model of Down syndrome, Hippocampus 13 (8) (2003) 905–914.
[32] S. Wergeland, Ø. Torkildsen, K.M. Myhr, et al., Dietary vitamin D3 supplements reduce demyelination in the cuprizone model, PLoS One 6 (10) (2011) e26262.
[33] R. Fu, X. Ma, Z. Bian, et al., Digital separation of diaminobenzidine-stained tissues via an automatic color-filtering for immunohistochemical quantification, Biomed. Opt. Express 6 (2) (2015) 544–558.
[34] A.C. Ruifrok, D.A. Johnston, Quantification of histochemical staining by color deconvolution, Anal. Quant. Cytol. Histol. 23 (4) (2001) 291–299.
[35] V.M. Mora-Bautista, Congenital anomalies of the kidney and the urinary tract in Down syndrome children, Rev. Colomb. Nefrol. 5 (1) (2018) 54–60.
[36] C. Niamien-Attai, J. Bacchetta, B. Ranchin, et al., Renal abnormalities in Down syndrome: a review, Arch. Pediatr. 24 (10) (2017) 1013–1018.
[37] D. Hartley, T. Blumenthal, M. Carrillo, et al., Down syndrome and Alzheimer's disease: common pathways, common goals, Alzheimers Dement. 11 (6) (2014) 700–709.
[38] Y.F. Shea, L.W. Chu, M.Y. Mok, et al., Amyloid beta 1-42 and tau in the cerebrospinal fluid of renal failure patients for the diagnosis of Alzheimer's disease, J. Nephrol. 27 (2) (2014) 217–220.
[39] Y.H. Liu, Y. Xiang, Y.R. Wang, et al., Association between serum amyloid-beta and renal functions: implications for roles of kidney in amyloid-beta clearance, Mol. Neurobiol. 52 (1) (2015) 115–119.
[40] Y. Xiang, X.L. Bu, Y.H. Liu, et al., Physiological amyloid-beta clearance in the periphery and its therapeutic potential for Alzheimer's disease, Acta Neuropathol. 130 (4) (2015) 487–499.
[41] E.C. Chow, M.R. Durk, C.L. Cummins, et al., 1Alpha,25-dihydroxyvitamin D3 upregulates P-glycoprotein via the vitamin D receptor and not farnesoid X receptor in both fxr(−/−) and fxr(+/+) mice and increased renal and brain efflux of digoxin in mice in vivo, J. Pharmacol. Exp. Ther. 337 (2011) 846–859.
[42] T.V. Patel, A.K. Singh, Role of vitamin D in chronic kidney disease, Semin. Nephrol. 29 (2) (2009) 113–121.
[43] I. Lopez, F.J. Mendoza, Aguilera-Tejero, et al., The effect of calcitriol, paricalcitol, and a calcimimetic on extraosseous calcifications in uremic rats, Kidney Int. 73 (3) (2008) 300–307.
[44] P. Mao, P.H. Reddy, Aging and amyloid beta-induced oxidative DNA damage and mitochondrial dysfunction in Alzheimer's disease: implications for early intervention and therapeutics, Biochim. Biophys. Acta 1812 (11) (2011) 1359–1370.
[45] K. Tsuzuki, R. Fukatsu, Y. Hayashi, et al., Amyloid beta protein and transthyretin, sequestrating protein colocalize in normal human kidney, Neurosci. Lett. 222 (3) (1997) 163–166.
[46] F.K. Wiseman, L.J. Pulford, C. Barkus, et al., Trisomy of human chromosome 21 enhances amyloid-β deposition independently of an extra copy of APP, Brain 141 (2018) 2457–2474.
[47] F.C. Gomes, M.F. Mattos, E.M. Goloni-Bertollo, E.C. Pavarino, Alzheimer's disease in the Down syndrome: an overview of genetics and molecular aspects, Neurol. India (2018) (Situation: Pre-Acceptance proof).
[48] V.P. Prasher, et al., Molecular mapping of Alzheimer-type dementia in Down's syndrome, Ann. Neurol. 43 (1998) 380–383.
[49] J. Beer, C.L. Masters, K. Beyreuther, Cells from peripheral tissues that exhibit high APP expression are characterized by their high membrane fusion activity, Neurodegeneration 4 (1) (1995) 51–59.
[50] M.O. Grimm, J. Mett, C.P. Stahlmann, et al., Neprilysin and Aβ clearance: impact of the APP intracellular domain in NEP regulation and implications in Alzheimer's disease, Front. Aging Neurosci. 5 (98) (2013) 1–27.
[51] H. Shi, A.W. Norman, Okamura WH, et al. 1alpha,25-Dihydroxyvitamin D3 modulates human adipocyte metabolism via nongenomic action, FASEB J. 15 (14) (2001) 2751–2753.
[52] D. Gezen-Ak, I.L. Atasoy, E. Candaş, et al., Vitamin D receptor regulates amyloid Beta 1-42 production with protein disulfide isomerase A3, ACS Chem. Neurosci. 8 (10) (2017) 2335–2346.
[53] A. Lo, H.G. Brown, B.A. Fivush, et al., Renal disease in Down syndrome: autopsy study with emphasis on glomerular lesions, Am. J. Kidney Dis. 31 (2) (1998) 329–335.
[54] I. Ariel, T.R. Wells, B.H. Landing, et al., The urinary system in Down syndrome: a study of 124 autopsy cases, Pediatr. Pathol. 11 (1991) 879–888.
[55] I.N. Sergeev, Q. Song, High vitamin D and calcium intakes reduce diet-induced obesity in mice by increasing adipose tissue apoptosis, Mol. Nutr. Food Res. 58 (6) (2014) 1342–1348.
[56] C. Duggan, J. de Dieu Tapsoba, C. Mason, et al., Effect of vitamin D3 supplementation in combination with weight loss on inflammatory biomarkers in postmenopausal women: a randomized controlled trial, Cancer Prev. Res. (Phila.) 8 (7) (2015) 628–635.
[57] S.J. Rosenstreich, C. Rich, W. Volwiler, Deposition in and release of vitamin D3 from body fat: evidence for a storage site in the rat, J. Clin. Invest. 50 (3) (1971) 679–687.
[58] R. Nair, A. Maseeh, Vitamin D: the “sunshine” vitamin, J. Pharmacol. Pharmacother. 3 (2) (2012) 118–126.
[59] T.T. Rohn, E. Head, Caspases as therapeutic targets in Alzheimer's disease: is it time to “cut” to the chase? Int. J. Clin. Exp. Pathol. 2 (2) (2008) 108–118.
[60] S. Gowda, P.B. Desai, S.S. Kulkarni, et al., Markers of renal function tests, N. Am. J. Med. Sci. 2 (4) (2010) 170–173.
[61] T. de Jesus Soares, R.A. Volpini, H.D. Francescato, et al., Effects of resveratrol on glycerol-induced renal injury, Life Sci. 81 (8) (2007) 647–656 2.
[62] V. Landel, C. Annweiler, P. Millet, et al., Vitamin D, cognition and Alzheimer's disease: the therapeutic benefit is in the D-tails, J. Alzheimers Dis. 53 (2) (2016) 419–444.
[63] F.C. Lam, R. Liu, P. Lu, et al., Beta-Amyloid efflux mediated by p-glycoprotein, J. Neurochem. 76 (4) (2001) 1121–1128.
[64] K.S. Crider, T.P. Yang, R.J. Berry, et al., Folate and DNA methylation: a review of molecular mechanisms and the evidence for folate's role, Adv. Nutr. 3 (1) (2012) 21–38.